JOURNAL OF MATERIALS SCIENCE 24 (1989) 915–920

Study of the effect of heat treatment on hydrogen embrittlement of AISI 4340 steel

E. QUADRINI
Dipartimento di Scienze dei Materiali e della Terra, Università di Ancona, Via Brecce Bianche, 60131 Ancona, Italy

Delayed failure tests were performed on fully-quenched AISI 4340 steel tempered at 500 and 700° C, subjected to sustained tensile loads and cathodically charged with hydrogen (current density 10 mA cm^{-2}) in an aqueous solution of 0.1 N sulphuric acid. The aim was to study the effect of the microstructure on the behaviour of steel towards the embrittling action of hydrogen. The tests were carried out with two different research techniques in order to highlight this behaviour better. This was done with a view to making the use of the steel safer. With the methods used the results obtained, although substantially different from each other, showed that thermodynamically more stable structures are less sensitive to the phenomenon of hydrogen embrittlement.

1. Introduction

The detrimental effect which hydrogen produces in metals, generally known as hydrogen embrittlement, has been the subject of numerous studies [1–7]. This has always been one of the central problems of practical and theoretical material technology, of corrosion and protection of metals and of metal physics.

Hydrogen is the cause of damage whenever metal–hydrogen systems are involved in the production, transport and storage of hydrogen, or fluids containing hydrogen, and in the presence of electrochemical processes such as pickling, galvanic electrodeposition, cathodic protection and corrosion.

Unlike what normally happens in other cases of embrittlement, that provoked by hydrogen occurs in static load conditions and with a stress considerably below the yield point. High-resistance steels are particularly sensitive to this phenomenon [8–11].

Various theories have been proposed to explain the mechanism by which hydrogen carries out its detrimental action. Among these the most accredited are the following.

1.1. The pressure theory

This theory, which is the oldest, was proposed by Zapffe and Sims [12] and subsequently modified by Tetelman [13]. It attributes the hydrogen embrittlement phenomenon to the strong pressures which arise inside the microvoids present in the material after the transformation of atomic hydrogen into molecular hydrogen.

However, this theory cannot explain those embrittlement phenomena found in materials exposed to low hydrogen pressures (P_{H_2} = 1 atm). Indeed, in these cases, since the pressure inside the microvoids is unable to overcome the outside pressure it is insufficient to cause the formation of cracks.

1.2. The decohesion mechanism

According to this model, proposed by Troiano and colleagues [14–17], atomic hydrogen gathering at the apex of the microcracks, where the plastic deformations are largest, reduces the interatomic cohesion forces.

While this theory explains very well the embrittlement phenomena which occur with intergranular and cleavage-type fractures, it is difficult to reconcile with those cases in which the fracture surfaces are dome-shaped (presence of plastic deformations).

1.3. Surface energy theory

This theory, proposed by Petch and Stables [18], like the one above refers to the presence of microcracks inside the material. In this case, however, it is the presence of the hydrogen absorbed on the inside surface of the microcrack which reduces the surface energy.

This model appears contradictory too. Indeed, in the cases in which hydrogen cannot be absorbed quickly at the apex of the crack, the crack's growth should be discontinuous. However, this has rarely been observed.

Another model attributes a material's loss of ductility to the temporary or permanent interaction of hydrogen which spreads with the dislocations, inclusions and microcavities, point faults and grain joints [19–21]. These faults constitute excellent traps for hydrogen atoms. In this case too, however, it is impossible to explain all the phenomena without running into conflicting interpretations.

Indeed, while some cases of embrittlement can be explained by supposing that atomic hydrogen obstructs the movement of the dislocation (the case of the fragile fractures), other cases are explained by attributing to hydrogen the capacity to facilitate

0022–2461/89 $03.00 + .12

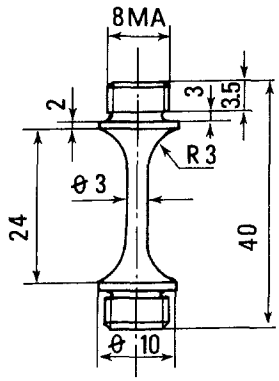

Figure 1 Specimen geometry (dimension in millimetres).

the movement of the dislocations (the case of ductile fractures).

Since none of these theories can explain on its own the complex phenomena which determine the behaviour of a material towards the embrittling action of hydrogen, it is logical to think of a simultaneous action of the various mechanisms.

In the author's Department a research programme is in progress which aims to examine the embrittling influence of hydrogen on two types of steel (AISI 4140 and AISI 4340) in order to determine the effect of environmental and metallurgical variables. Two previous papers [22, 23] referred to studies made by varying the specimen geometry and the primary austenitic grain size of a fully quenched steel subjected to hydrogen embrittlement tests.

This paper reports the results of delayed failure tests on samples of a fully quenched AISI 4340 tempered at two different temperatures. Indeed, the phenomenon through which hydrogen spreads and accumulates on the inside of a crystalline structure is closely related to the microstructure.

The failure tests are carried out following different techniques which can be classified like this:

(i) tests on smooth specimens with constant load and strain, with or without cracks or notches [24];

(ii) tests on smooth specimens obtained at a low and constant strain speed, with or without cracks or notches [25, 26];

(iii) tests on mechanical-type specimens of the fracture with serious faults obtained by fatigue precracking with constant load or strain [27–29].

On comparing the results obtained with these methods substantial differences were found in the values of the threshold loads and of the fracture incubation times. Therefore, in order better to define the field of use of the new steel and so make it safer, the tests were carried out with different load application methods.

TABLE I Chemical composition of steel used (wt %)

C = 0.40	Cu = 0.17	Mn = 0.75
Ni = 1.74	Si = 0.26	Sn = 0.022
Cr = 0.81	P = 0.019	Al = 0.028
Mo = 0.23	S = 0.015	

2. Experimental procedure

The chemical composition of AISI 4340 steel used in this work is reported in Table I. The sample geometry and dimensions as regards length and gauge length are reported in Fig. 1.

After mechanical preparation the specimens were quenched in a tubular oven provided with a constant supply of argon. The vertical oven also enabled us to achieve extremely drastic quenching, since a special specimen-releasing device allowed the specimen to reach a quenching bath very rapidly. The heat treatment was carried out through austenitizing for one hour at 870° C, followed by oil-quenching.

After the quenching treatment a part of the specimens was tempered at 500 and 700° C. The metallographic structures of the sample after the different heat treatments are reported in Fig. 2.

The homogeneity of the heat treatment was checked by subjecting all the samples to Rockwell C hardness tests: the values obtained together with the other mechanical characteristics are reported in Table II.

An influence of surface finishing on the results obtained in delayed failure tests was found in a recent work [30]. In order to reduce this effect as much as possible, therefore, a check was made of the sample surfaces by means of Perthen Perthometer C5D electronic roughness measuring apparatus. In Fig. 3 the averge roughness profile obtained from these measurements is reported.

The hydrogen embrittlement tests were carried out at the temperature of 22 ± 1° C. Indeed, this is generally the temperature at which steels similar to ours show their greatest sensitivity to hydrogen embrittlement.

Hydrogen was introduced into the material with the cathodic load procedure, using an aqueous solution 0.1 N H_2SO_4 in contact with the atmosphere. This operation was carried out in a double-walled glass cylinder in whose cavity the thermostatic liquid circulated. Inside the cylinder the sample which constituted the cathode was assembled, while a platinum coil wrapped round it at a distance of 2 cm acted as a controelectrode.

The hydrogen charge occurred in intensiostatic conditions, that is at a prefixed and constant current value: in our tests this current density value was about 10 mA cm^{-2}. In these conditions the sample assumed a potential of complete cathodic protection and the only phenomenon possible was hydrogen discharge.

The sustained tensile load tests were carried out with two different load application methods. In one series of tests the load was applied 60 min before hydrogen discharge, while in a second series the

TABLE II Mechanical properties of steel used

Heat treatment	Hardness (HRC)	Yield strength (MPa)	Ultimate tensile strength (MPa)
Oil-quenched	55	1650	2050
Tempered at 500° C	44	1100	1250
Tempered at 700° C	32	700	860

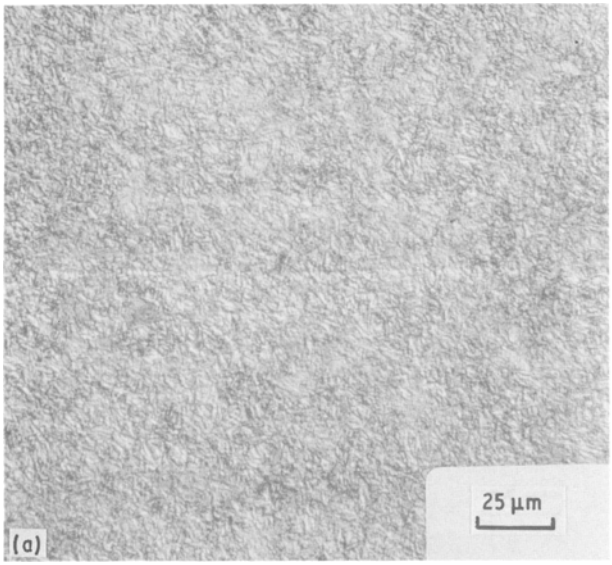

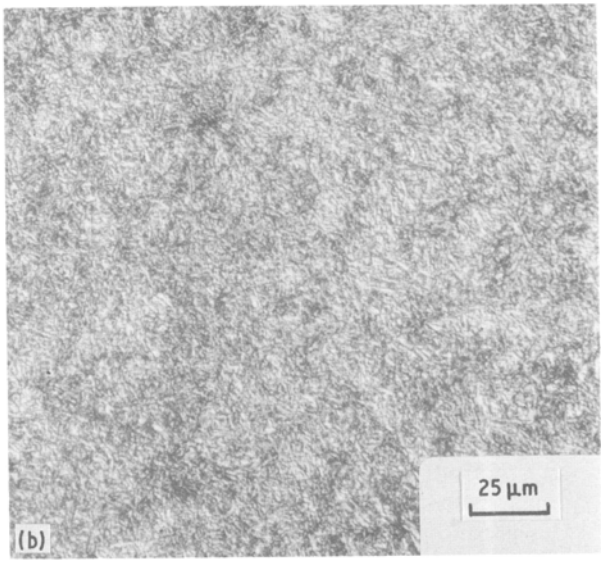

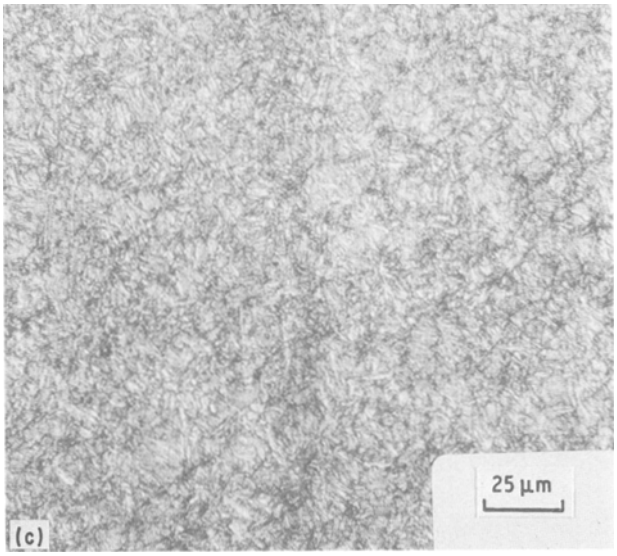

Figure 2 Metallographic aspect of the steel used: (a) oil-quenched, (b) oil-quenched and tempered at 500° C, (c) oil-quenched and tempered at 700° C.

hydrogen discharge preceded load application by 60 min.

The tests which did not reach failure in 150 to 200 h were interrupted since this is a long enough time to ascertain the threshold load.

3. Results and discussion

Figs 4 and 5 report the results of the sustained tensile load tests carried out on fully quenched AISI 4340 steel tempered at 500 and 700° C. The results in Fig. 4 were obtained in the tests in which the stress application occurred 60 min before hydrogen discharge, while the results in Fig. 5 were obtained by applying the stress 60 min after this discharge.

The trend of these curves leads to two interesting observations: firstly that the results depend to a great extent on the research technique, and secondly that structures obtained in conditions close to thermodynamic equilibrium are less sensitive to hydrogen embrittlement.

Among the various theories proposed to explain the phenomena which determine the behaviour of a material towards the embrittling action of hydrogen (of which there is a brief list in Section 1), those which seem to us most suitable for interpreting our results are the dislocation theory [20, 21] and the hydrogen trap theory [31], which is an integral part of the first.

According to these theories, hydrogen atoms, given their modest dimensions (0.104 nm), while spreading in the structure of a material divide themselves between the dislocations and the microcavities present on the grain boundaries and in the interstitial positions. These faults, always present in the crystal lattice, constitute excellent traps for these atoms.

During plastic deformation the dislocations transport the hydrogen atoms into the zones of greatest triaxal stress. In these zones hydrogen accumulates and damages their mechanical characteristics until, on reaching a critical concentration, the plastic zone fractures and the cycle continues.

In untempered martensite the high number of dislocations present in the highly distorted lattice encourages the transport and the accumulation of hydrogen. In a structure of this kind, therefore, the time necessary for hydrogen to saturate a potential fault is greater and the nucleation of the fracture occurs in a shorter time (leftward movement of the curves of Figs 4 and 5).

In addition, the lengthened shape of its crystals

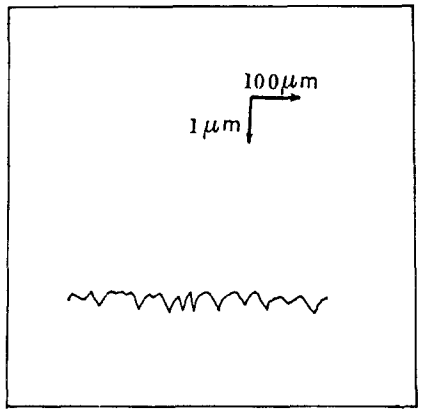

Figure 3 Roughness profile.

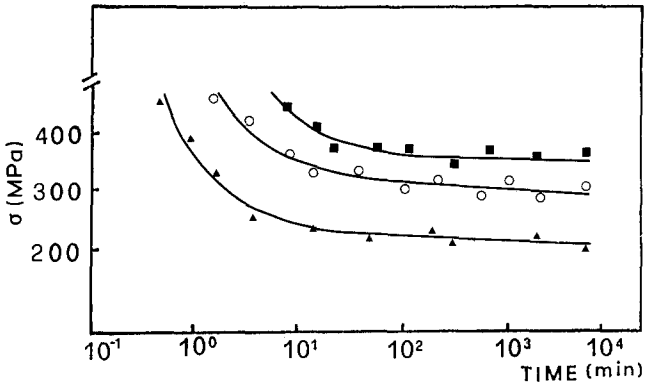

Figure 4 Effect of the heat treatment on time to failure: tests in which the stress occurred 60 min before hydrogen discharge. (▲) oil-quenched, (●) oil-quenched and tempered at 500° C, (■) oil-quenched and tempered at 700° C.

makes this structure particularly favourable to the propagation of the fracture, which with the same hydrogen content, occurs at lower levels of stress (downward movement of the curves in Figs 4 and 5).

The same considerations explain why structures obtained by high-temperature tempering of martensite are less sensitive to hydrogen embrittlement. In these thermodynamically more stable structures the number of dislocations is relatively low and therefore the time needed for hydrogen to accumulate and nucleate the fracture is greater (rightward movement of the curves in Figs 4 and 5).

In addition, with this heat treatment martensite is transformed, forming globular cementite, whose particles, which get less and less fine as the temperature increases, obstruct the growth of the fracture. This will only manifest itself if subjected to greater stress (upward movement of the curves in Figs 4 and 5).

As regards the differences which emerged in the tests carried out with the two research techniques, they can be attributed to the mechanisms by which the hydrogen atoms transported by the dislocations interact with the traps present in the metal lattice. These mechanisms depend substantially on the energy with which these interactions occur [32] and on the presence or absence of hydrogen in the traps at the moment of stress application.

If the value of this energy enables the dislocations to remove the hydrogen present in the traps, these traps will behave as sources of hydrogen (reversible traps); otherwise their behaviour is comparable to that of a harmless reservoir (irreversible traps).

In tests carried out applying stress to the samples saturated with hydrogen, the dislocations during their movement absorb the hydrogen contained in the reversible traps, whose energy is smaller. In this way the critical concentration in a potential fault is reached sooner and the fracture nucleation time will be shorter (leftward movement of the curves of Figs 4 and 5).

It is clear that in these tests, since the irreversible traps are already saturated with hydrogen at the moment when the load is applied and the hydrogen contained in them cannot be removed, they will have no possibility of interacting with the dislocations.

Exactly the opposite occurs in the tests in which the stress is applied before the hydrogen discharge. Indeed, in these tests, since at the moment of load application the traps are empty, the hydrogen transported by the dislocations is released into the irreversible traps because their interaction energy is greater. In this way the critical concentration of hydrogen in a potential fault is reached later and fracture nucleation is delayed (rightward movement of the curves of Figs 4 and 5). While these considerations justify the delays in fracture nucleation and propagation, they do not explain the lower threshold load values.

In order to explain this behaviour, we must consider the phenomena which determines the behaviour of a material at the moment when it is subjected to stress. Creep phenomena of very modest proportions occur in the material during load application, and in particular at points corresponding to already existing micronotches on the surface, where the stress is greater. As a consequence of the deformations, stress relaxation phenomena are induced in the crack tip at a rate decreasing with time.

During these deformations cavitation phenomena occur in the sites in which the local stress reaches the critical value and consequently there is a release of tension at the crack tip. In this way at every moment of load application there is an increase both in the

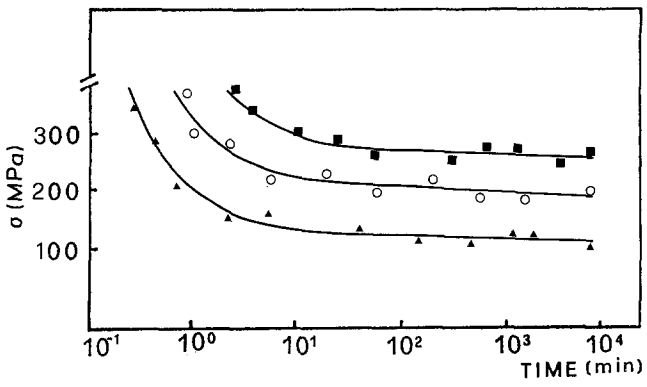

Figure 5 Effect of the heat treatment on time to failure: tests in which the stress occurred 60 min after hydrogen discharge. (▲) oil-quenched, (○) oil-quenched and tempered at 500° C, (■) oil-quenched and tempered at 700° C.

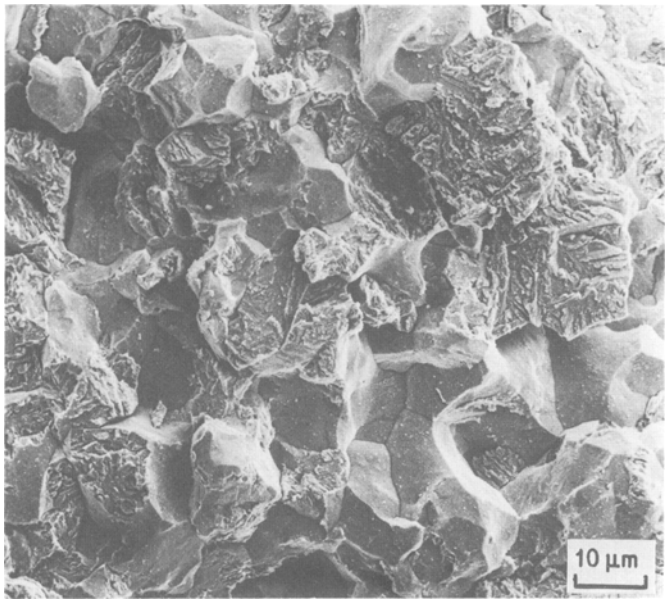

Figure 6 SEM fractgraphy with both intergranular and quasi-cleavage fracture.

microvoid population and in the sites with subcritical stress values. Some of these sites have a value very close to the stress necessary to cause cavitation.

Some authors suppose [33, 34] that during the initial relaxation phenomenon the number of subcritically stressed sites decreases with time. If the material is already saturated with hydrogen at the moment when these relaxation phenomena occur, the sites which in the absence of hydrogen were under subcritical stress, in the presence of hydrogen reach the critical stress with subsequent nucleation of microvoids because of the decrease in local cohesive strength. The presence of these microvoids, as well as facilitating hydrogen diffusion in front of the crack tip, weakens the resistance of the material and facilitates delayed fracture.

If the load application precedes cathodic polarization, when hydrogen diffuses in the material the relaxation phenomenon is practically exhausted. In this way the number of microvoids under subcritical stress will be lower, with a consequent reduction in local stress at the crack tip. In these conditions hydrogen diffusion and fracture nucleation will take longer and the stress necessary to cause fracture is greater compared with that required by precharged material.

From examination of the fractographs of Fig. 6 a predominantly intergranular type failure can be seen with limited areas of quasi-cleavage. This morphology, which is typical of the fragile fracture induced by hydrogen, does not seem to be modified by heat treatment.

4. Conclusions

The experimental results confirm that structures obtained in conditions closer to those of equilibrium are less sensitive to hydrogen embrittlement.

The results showed a considerable dependence on the techniques with which the survey was carried out. This behaviour was attributed to the different mechanisms by which the hydrogen transported by the dislocations interacts with the traps present in the metallic lattice, and to those creep phenomena which occur in the material at the moment when it is subjected to stress.

A comparative examination of these results with those obtained with other investigative techniques points to the necessity of programming a series of tests in order to avoid excessively conservative or unsafe choices.

The results of the fractographic study highlighted a predominantly intergranular fracture type.

References

1. I. M. BERNSTEIN and A. W. THOMPSON, *Int. Met. Rev.* **21** (1976) 269.
2. J. E. COSTA and A. W. THOMPSON, *Metall. Trans. A* **12A** (1981) 761.
3. D. C. LANGSTAFF, G. MEYRICH and J. P. HIRTH, *Corrosion* **37** (1981) 429.
4. V. N. ZIKEEV, *Metalloved, Term. Obrab. Met.* **5** (1982) 18.
5. J. B. GREER, *Mat. Perform.* **14** (1975) 11.
6. G. BIGGIERO, A. BORRUTO and F. CARAFA, *Metallurgia Italiana* **3** (1984) 166.
7. V. A. MARICHEV, *Werkst. Korrosion* **33** (1982) 1.
8. M. ELICES, G. MAEDER and V. SANCHEZ, *Br. Corros. J.* **18** (1983) 80.
9. M. CORNET, W. RACZYNSKI and S. TALBOT-BESNARD, *Mém. Sci. Rev. Mét.* **69** (1) (1972) 27.
10. M. CORNET, J. L. DILLARD and S. TALBOT-BESNARD, *ibid.* **69** (10) (1972) 689.
11. J. P. FIDELLE, R. BRODEUR and C. ROUX, in Proceedings of an International Conference, Bruieres-le-Chatel, edited by A. W. Thompson and I. M. Bernstein (1976) pp. 507–515.
12. C. ZAPFFE and C. SIMS, *AIME Trans.* **145** (1941) 225.
13. A. S. TETELMAN, "Fundamental Aspects of Stress Corrosion Cracking", edited by R. W. Staehle, A. J. Forty and D. Van Rooyen, NACE-1 (1969) pp. 446–464.
14. R. P. FROHMBERG, W. J. BARNETT and A. R. TROIANO, *Trans. ASM* **47** (1955) 892.
15. H. H. JOHNSON, J. G. MORLET and A. R. TROIANO, *Trans. TMS-AIME* **212** (1958) 528.
16. E. A. STEIGERWALD, F. W. SCHOLLER and A. R. TROIANA, *ibid.* **215** (1959) 1048.
17. A. R. TROIANO, *Trans. ASM* **52** (1960) 54.
18. N. O. PETCH and P. STABLES, *Nature* **169** (1952) 842.
19. G. E. KERNS, M. T. WANG and R. W. STACHLE, "Stress Corrosion Cracking and Hydrogen Embrittlement of Iron Base Alloys", edited by R. W. Stachle, J. Hochmann,

R. D. McKnight and J. E. Slater, NACE-5 (1977) pp. 700–735.
20. G. M. PRESSOUYRE, J. DOLLET and B. VIEILLARD-BARON, *Etud. Sci. Rev. Mét.* **79** (5) 1982 227.
21. *Idem, Ibid.* **79** (41) (1982) 161.
22. E. QUADRINI and F. VENIALI, *Mater. Chem. Phys.* **10** (1984) 457.
23. E. QUADRINI, *ibid* **15** (1986) 155.
24. NACE Technical Practices Committee, Test Method, "Testing of metals for resistance on sulphide stress cracking at ambient temperature", NACE standard TM-01-77 (1977).
25. ASTM Special Technical Publication 610, edited by H. L. Craig, Jr, Philadelphia (1975).
26. ASTM Special Technical Publication 665, edited by G. M. Ugiansky and J. H. Payer, Philadelphia (1978).
27. ASTM Standard Test Method, "Plane-strain Fracture Toughness of Metallic Materials", ASTM Standard E 399-83 (American Society for Testing and Materials, Philadelphia, 1983).
28. S. R. NOVAK and S. T. ROLFE, *J. Mater.* **4** (1969) 701.
29. A. CIGADA and F. RE, *Rivista dell'Industria Chimica* **9** (1981) 21.
30. E. QUADRINI, R. FRATESI and G. ROVENTI, *Mater. Sci. Engng* **96** (1987) 51.
31. G. M. PRESSOUYRE, *Acta Metall.* **28** (1980) 895.
32. *Idem, Met. Trans. A* **10** (1979) 1571.
33. R. A. ORIANI and P. H. JOSEPHIC, *Acta. Metall.* **27**, 997.
34. *Idem, ibid.* **29** (1981) 660.

Received 9 November 1987
and accepted 1 March 1988